Sensors & Transducers, Vol. 179, Issue 9, September 2014, pp. 79-86

Sensors & Transducers

Modeling, Simulation and Experimental Research on Brushless Doubly-Fed Machine

[1] Xiao Yiping, [2] Wang Xuefan
[1] School of Electrical and Electronic Engineering, Hubei University of Technology, Wuhan, Lizhi Road, 430068, China,
[2] School of Electrical and Electronic Engineering, Huazhong University of Science &Technology, Wuhan, Luoyu Road, 430074, China
[1] E-mail: yp_xiao2013@163.com

Received: 11 June 2014 /Accepted: 29 August 2014 /Published: 30 September 2014

Abstract: The conventional doubly-fed induction generator (DFIG) requires brushes and copper slip-rings which needs extra maintenance, produces noises and decreases system's stability. In this paper, a pole-changing wound rotor brushless doubly-fed machine (BDFM) with an optimized rotor design is studied. It applies the theory of the winding tooth harmonic and the pitch of the rotor winding can be adjusted flexibly. It not only improves the winding coefficient and reduces the magnetomotive force harmonic. It has high utilization rate and lower harmonic content. The modeling and simulation of BDFM is completed. Experimental results obtained from a 64 kW prototype of a pole-changing BDFM are presented and fully discussed. Experimental studies including output voltage characteristic and load response under the three different speed modes have demonstrated performance advantages of the pole-changing BDFM. *Copyright © 2014 IFSA Publishing, S. L.*

Keywords: Brushless doubly-fed machine (BDFM), Modeling, Simulation, Experiment.

1. Introduction

The Doubly-fed induction generator (DFIG) is widely applied in energy conversion systems such as wind turbines or pump-alike installations [1]. However, brushes and copper slip-rings are required in the conventional DFIG. The use of brushes needs extra maintenance, produces noises and decreases system's stability [2]. Therefore, a brushless doubly-fed machine (BDFM) is presented.

The BDFM is a better alternative to the DFIG for wind turbines or pump-alike applications. The main advantages of this brushless machine are less maintenance, no noises and better stability. This is particularly suitable for wind turbines applications located in remote areas. A power converter which connected with the machine windings has much less power than the machine rated power. In addition, BDFM has a possibility of improving power factor and compensating reactive power. Its operational mode is flexible. It can function as either an induction motor or as a classical generator which called brushless doubly-fed generator (BDFG) [3-7].

The report about BDFM in the literature was in the early twentieth century [8]. The first BDFM includes two doubly-fed induction machines connected to the same shaft. It is called cascaded BDFM. An improvement to the cascaded BDFM is called self-cascaded BDFM. In the implementations of self-cascaded BDFM, there are two stator windings without any direct magnetic coupling between them [9]. In China, reluctance rotor brushless doubly-fed machine was studied by Shenyang University of Technology in the 1980s.

The reluctance rotor BDFM is high efficient [10]. And cage BDFM was discussed in some universities such as Zhejiang University etc. The cage BDFM has simple structure, reasonable cost and is easily made [11]. But the harmonic contents in the windings current of two types of BDFM mentioned above are both large. Besides, A wound rotor BDFM was proposed by Huazhong University of Science and Technology [12].

In this paper, a pole-changing wound rotor BDFM (PCBDFM) with an optimized rotor design is studied. It applies the theory of the winding tooth harmonic and the pitch of the rotor winding can be adjusted flexibly [13]. It not only improves the winding coefficient, but also reduces the magnetomotive force harmonic. It has high utilization rate and lower harmonic content [14].

2. Proposed Approach

2.1. Structure of PCBDFM

In the implementations of a pole-changing wound rotor BDFM (Fig. 1), there are two stator windings with different numbers of poles. One of the stator windings called control winding is used as excitation source and the other called power winding is connected to the grid. The control winding is fed by a frequency inverter which is designed for 20 %-30 % of the machine rated power. The rotor is designed to magnetically be coupled with two stators. The main characteristic of this topology can be described as only one machine with two stators and one rotor [15]. The frequency inverter is either a back-to-back converter or a matrix converter which is controlled by controller. The filter is composed by resistors, inductors, and capacitors connected together in order to filter the harmonic from the grid.

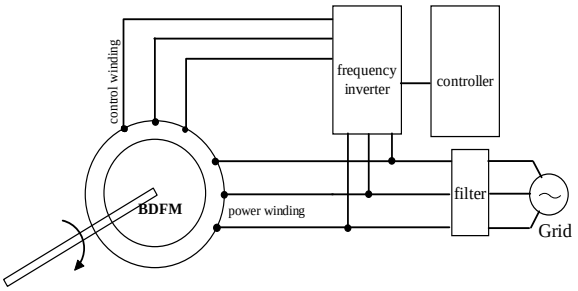

Fig. 1. Brushless doubly-fed machine structure diagram.

The stators with different number of poles have two topologies: single-stage topology and dual-stage topology. The single-stage topology is only one stator but two different output terminals. Looking from different terminals, the equivalent stator poles number is different. The dual-stage topology is two separate stators with different number of poles located in the same stator slot. And the two stators are designed into different layers, pitches and branches. The rotor is a closed winding with two layers structure. Its induced current can create rotating magnetic field with two different poles number and opposite direction. The stators/rotor winding design applies the theory of the winding tooth harmonic and the pitch of the rotor winding can be adjusted flexibly [13]. This design not only improves the winding coefficient, but also reduces the magnetomotive force harmonic.

2.2. Brushless Doubly Fed Machine Model

In order to understand the operating principle of the BDFG, it is necessary to be familiar with dynamic math model and unusual torque producing mechanism of the BDFM. The BDFG is represented by its rotor resistance, stators resistance, main magnetizing inductance, leakage inductance and mutual inductance.

Defining the stator and rotor inductances of the machine as:

$$\begin{aligned} L_p &= L_{\sigma p} + 3L_{mp} / 2 \\ L_c &= L_{\sigma c} + 3L_{mc} / 2 \\ L_r &= L_{\sigma r} + 3L_{mr} / 2 \\ M_{pr} &= 3L_{pr} / 2 \\ M_{cr} &= 3L_{cr} / 2, \end{aligned} \tag{1}$$

In Eq. (1)-(4), the subscripts "*p*", "*c*", "*r*" are used to indicate a variable related to the power winding/control winding /rotor winding of the BDFM. $L_{\sigma p}$, $L_{\sigma c}$, $L_{\sigma r}$ are the stators/rotor main magnetizing inductance of the machine, L_{mp}, L_{mc}, L_{mr} are the stators/rotor leakage inductance of the machine. L_p, L_c, L_r are the stators/rotor inductance of the machine, L_{pr}, L_{cr} are the stators/rotor mutual inductance of the machine. Using synchronous speed d-q coordinates, the machine voltage balance equations are [16]:

$$\dot{U}_p = (r_p + j\omega_p L_p)\dot{I}_p + j\omega_p M_{pr}\dot{I}_r, \tag{2}$$

$$\dot{U}_c = (r_c + j\omega_c L_c)\dot{I}_p + j\omega_c M_{cr}\dot{I}_r, \tag{3}$$

$$\begin{aligned} \dot{U}_r = 0 = (r_r + j(\omega_p - p_p\omega_r)L_r)\dot{I}_r + \\ j(\omega_p - p_p\omega_r)M_{cr}\dot{I}_c + j(\omega_p - p_p\omega_r)M_{pr}\dot{I}_p \end{aligned}, \tag{4}$$

In Eq. (2)-(4), ω_p, ω_c is the mechanical angular velocity of stators. ω_r is the mechanical angular velocity of rotor. p_p, p_c are the stators/rotor number of poles. r_p, r_c, r_r are the stators/rotor resistance of the machine.

When the machine is in a steady state, the relation of angular velocity of stators and rotor is shown in Eq.(5)

$$\omega_c = \omega_p - p_p\omega_r - p_c\omega_r, \quad (5)$$

From Eq.(5), changing ω_p and ω_c, then ω_r can be changed. This is the principle of the motor functioning. Similarly, changing ω_r and ω_c, then ω_p can be changed. This is the principle of the generator functioning. According to Eq.(5), Eq.(6) can be deduced.

$$\omega_r = \frac{\omega_p - \omega_c}{p_p + p_c}, \quad (6)$$

According to Eq.(6), if $\omega_c = 0$ (control winding current is DC), the BDFM runs at synchronous speed ($\omega_{syn} = \omega_p / (p_p + p_c)$). If $\omega_c > 0$ (current phase sequence of the control winding is the same as that of the power winding), then the machine is operated in sub-synchronous mode ($\omega_r < \omega_{syn}$), and if $\omega_c < 0$ (current phase sequence of the control winding is opposite to that of the power winding), then in super-synchronous model ($\omega_r > \omega_{syn}$).

Assuming the stators inner surface and rotor outer surface is smooth, air gap is uniform, three-phase stator windings and rotor winding is symmetric, the effect of magnetic hysteresis, saturating magnetic materials, and eddy current is ignored, using synchronous speed d-q coordinates, the BDFM matrix equations are [17]:

$$\begin{bmatrix} u_{pd} \\ u_{pq} \\ u_{cd} \\ u_{cq} \\ u_{rd} \\ u_{rq} \end{bmatrix} = \begin{bmatrix} r_p + L_p\rho & -\omega_p L_p & 0 & 0 & M_{pr}\rho & -\omega_p M_{pr} \\ \omega_p L_p & r_p + L_p\rho & 0 & 0 & \omega_p M_{pr} & M_{pr}\rho \\ 0 & 0 & r_c + L_c\rho & -\lambda_c L_c & M_{cr}\rho & -\lambda_c M_{cr} \\ 0 & 0 & \lambda_c L_c & r_c + L_c\rho & \lambda_c M_{cr} & M_{cr}\rho \\ M_{pr}\rho & -\lambda_r M_{pr} & M_{cr}\rho & -\lambda_r M_{cr} & r_r + L_r\rho & -\lambda_r L_r \\ \lambda_r M_{pr} & M_{pr}\rho & \lambda_r M_{cr} & M_{cr}\rho & \lambda_r L_r & r_r + L_r\rho \end{bmatrix} \begin{bmatrix} i_{pd} \\ i_{pq} \\ i_{cd} \\ i_{cq} \\ i_{rd} \\ i_{rq} \end{bmatrix} \quad (7)$$

In Eq. (7), ρ is the differential operator, $\lambda_c = (\omega_p - (p_p + p_c)\omega_r$, $\lambda_r = \omega_p - p_p\omega_r)$.

Using d-q coordinates, the electromagnetic torque of the machine can be expressed as [17]:

$$T_e = \frac{3}{2}P_p M_{pr}(i_{pq}i_{rd} - i_{pd}i_{rq}) - \frac{3}{2}P_c M_{cr}(i_{cq}i_{rd} - i_{cd}i_{rq}), \quad (8)$$

According to Eq.(8), the electromagnetic torque consists of two parts: the one part produced by interaction between the control winding current and the rotor winding current, and the other by interaction between the power winding current and the rotor winding current.

Using the model described in the Eq.(7) and Eq.(8), the BDFM can be simulated.

3. Simulation Results

Using Power System Blockset in Matlab/Simulink, according to the Eq.(7) and Eq.(8), the BDFM simulation model can be built. From the simulation model of the BDFM, the work features of the BDFM can be simulated.

When BDFM functions as motor (power is 10kW), L_p=0.0425, L_c=0.068, L_r=0.1054, M_{pr}=0.036, M_{cr}=0.0528, pp=7, pc=5, Up=220 V, fp=50 Hz, Uc=10, TL=20 N.m, the simulation wave of stators/rotor is shown as Fig. 2.

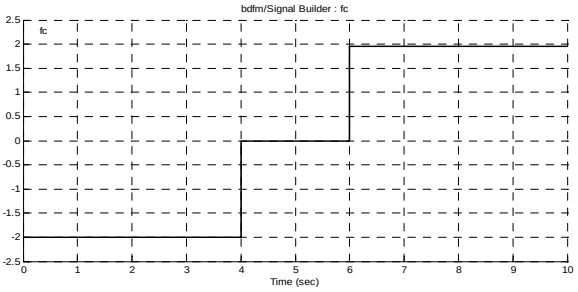

Fig. 2 (a). Given fc wave.

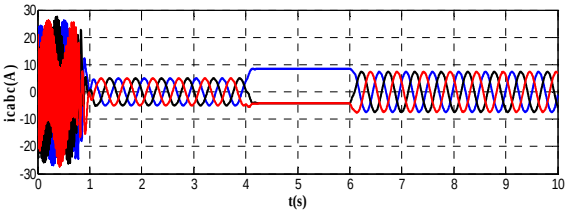

Fig. 2 (b). Control winding current wave.

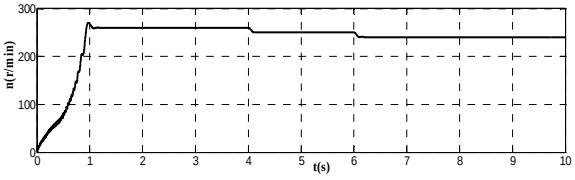

Fig. 2 (c). Rotor speed wave.

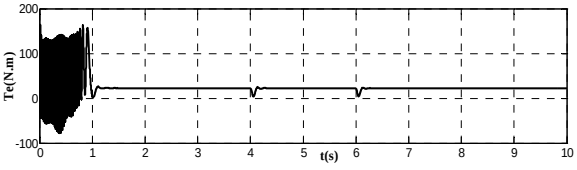

Fig. 2 (d). The electromagnetic torque wave.

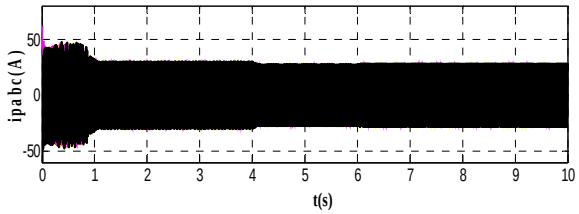

Fig. 2 (e). Power winding current wave.

From Fig. 2(c), Fig. 2 (d), when given fc as in Fig. 2(a), BDFM is operated in super-synchronous mode in 0-4 seconds (nr=260 r/min), and then in synchronous mode in 4-6 seconds (nr=250 r/min), finally in sub-synchronous mode in 6-10 seconds (nr=240 r/min), and the electromagnetic torque is about 22 N.m. From Fig. 2(b), the control winding current phase sequence in super-synchronous state is opposite to that in sub-synchronous state. From Fig. 2(e), power winding current frequency and amplitude is always stable except the initial impulse.

When BDFG functions as generator, the parameter of the BDFM is: the rated power P=64 kW, pp=4; pc=2; rp=0.074285; rc=0.11117; rr=0.83271; L_{pr}=0.064827; L_{cr}=0.21323; L_{mp}=0.02607; L_{mc}=0.0996; $L_{\sigma p}$=0.0010868; $L_{\sigma c}$=0.0010754; $L_{\sigma r}$=0.015798; L_{mr}=0.61784. Its synchronous rotor speed (nsyn) is 500 r/min. The simulation wave of stators/rotor is shown as Fig. 3.

From Fig. 3, when given rotor speed as in Fig. 3(a) and appropriate fc (in Fig. 3(b)) and uc (in Fig. 3(c)) or appropriate control winding current (in Fig. 3(d)), BDFG is operated respectively in sub-synchronous state (nr<nsyn (synchronous speed)), synchronous state (nr=nsyn), super-synchronous state (nr> nsyn).

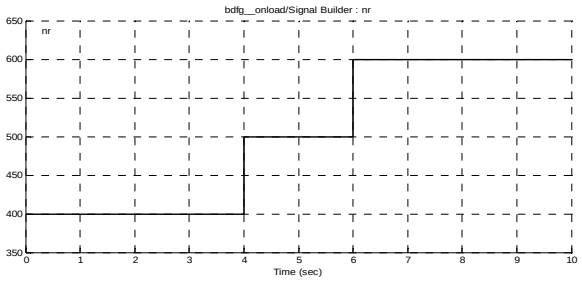

Fig. 3 (a). Given rotor speed (nr) wave.

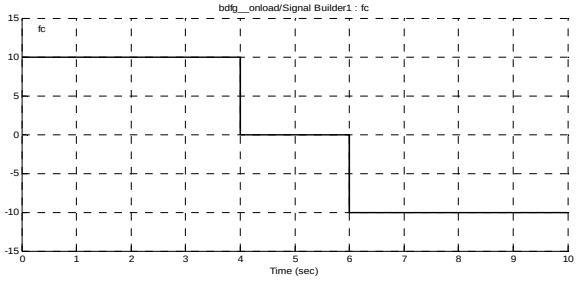

Fig. 3 (b). Given control winding frequency(fc) wave.

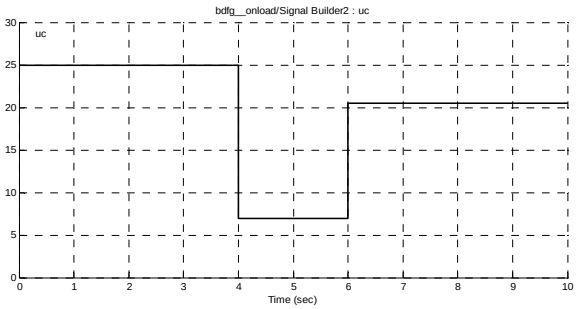

Fig. 3 (c). Given control winding voltage amplitude (uc) wave.

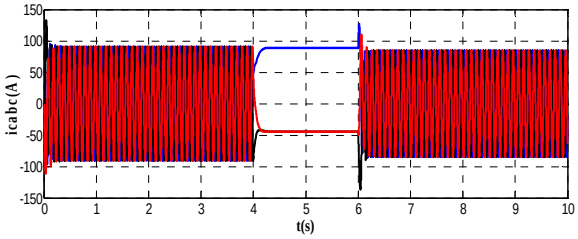

Fig. 3 (d). Control winding current wave.

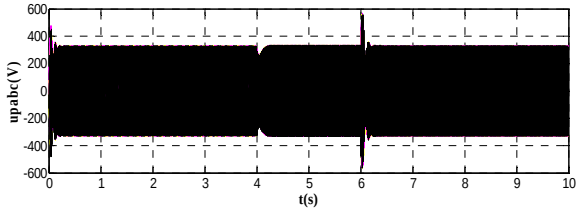

Fig. 3 (e). Power winding voltage wave.

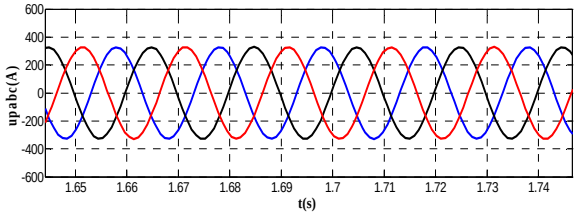

Fig. 3 (f). Power winding voltage wave during the period of 1.64 s-1.74 s.

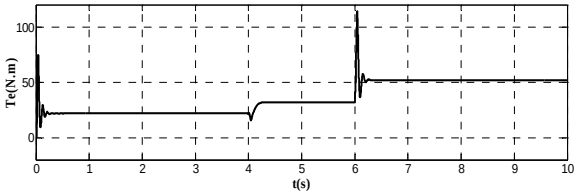

Fig. 3 (g). The electromagnetic torque wave.

Under the given nr, proper fc, and uc, the 64 kW BDFG's power winding voltage frequency is constantly 50 Hz and power winding phase voltage amplitude is continuously about 310 V (in Fig. 3(e) and (f)) in the three different modes, the same as the

grid frequency and phase voltage amplitude. In addition, as the rotor speed increases, the electromagnetic torque increases from 22 N.m, 32 N.m to 52 N.m (in Fig. 3(g)). Besides, according to Fig. 3, when the generator works at the three different modes, the output power winding voltage wave is sinusoidal wave nearly without harmonic content.

4. Experimental Results

Experimental BDFM prototype (in Fig. 4) power is 64 KW, its parameter is the same as the simulation model above (functioning as generator). The experimental BDFM runs in the generator mode. The prime motor is driven by wind turbine simulator. The control winding of BDFM is connected with an inverter and the power winding is connected with the grid.

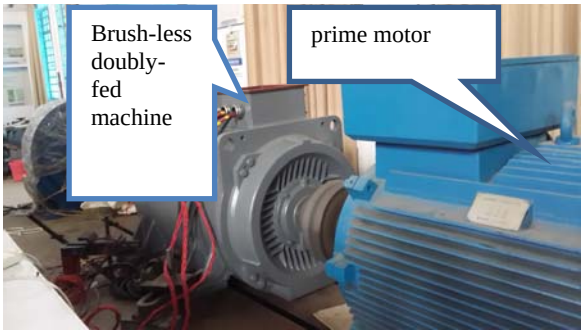

Fig. 4. Experimental prototype.

When wind turbine simulator drives the BDFG rotor to change the rotor speed from 600 r/min, 500 r/min to 400 r/min, the measured UV and VW line voltage wave and measured U, V phase current of control winding wave is shown in Fig. 5-Fig. 7.

From Fig. 5, when rotor speed is 600 r/min (in super-synchronous state), power winding line voltage effective value keeps constantly 400 V and its frequency keeps 50 Hz whether there is resistant load or motor load (in Fig. 5(b)-(d)) or not (in Fig. 5(a)) only by controlling the inverter to adjust the control current frequency (about 10 Hz) and amplitude in time (but the phase sequence of the control winding is opposite to that of the power winding). According to Fig. 5(a), Fig. 5(b) and Fig. 5(c), when load increases (from no-load to 30 kW resistant load) or decreases (from 30 kW resistant load to 6 kW resistant load), control current increases (from 80 A to 120 A) or decreases (from 120 A to about 85 A) correspondingly. When motor load is connected with the BDFG, there is a transient process (Fig. 5(d)), but power winding voltage amplitude and frequency is nearly invariable.

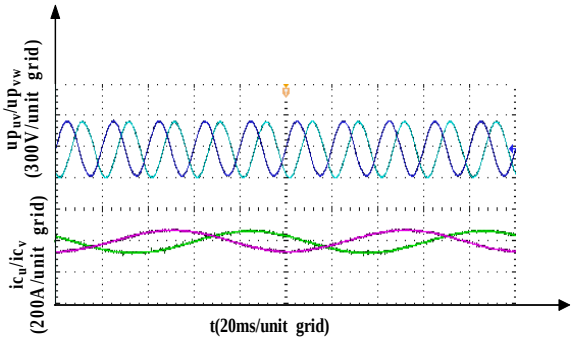

Fig. 5 (a). When rotor speed is 600 r/min, no-load output wave.

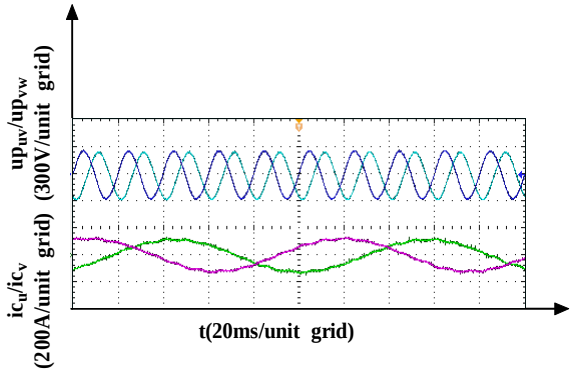

Fig. 5 (b). When rotor speed is 600 r/min, 30 kW resistance load steady-state output wave.

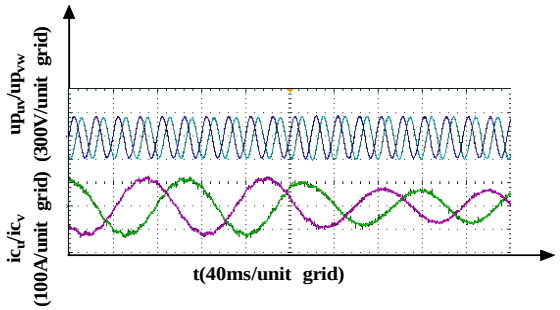

Fig. 5 (c). When rotor speed is 600 r/min, dynamic output wave when resistance load varying from 30 kW to 6 kW.

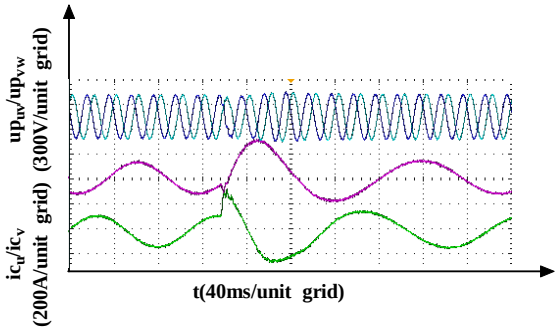

Fig. 5 (d). When rotor speed is 600 r/min, dynamic output wave when load varying from 30 kW resistance load to small motor load.

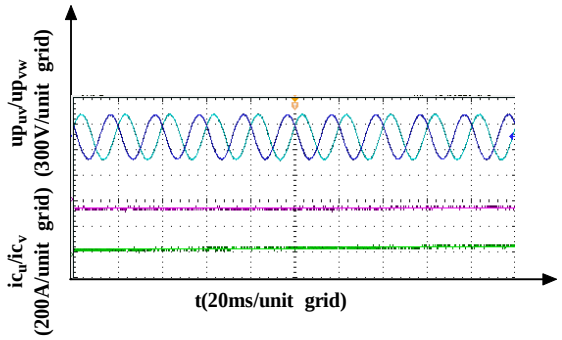

Fig. 6 (a). When rotor speed is 500 r/min, no-load output wave.

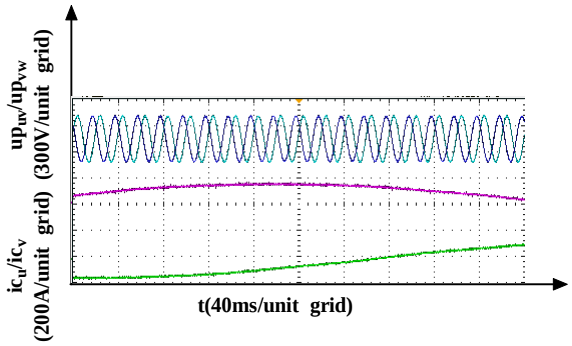

Fig. 6 (b). When rotor speed is 500 r/min, 30 kW resistance load steady-state output wave.

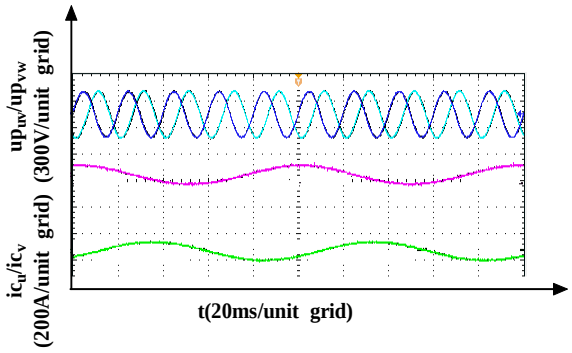

Fig. 7 (a). When rotor speed is 400 r/min, no-load output wave.

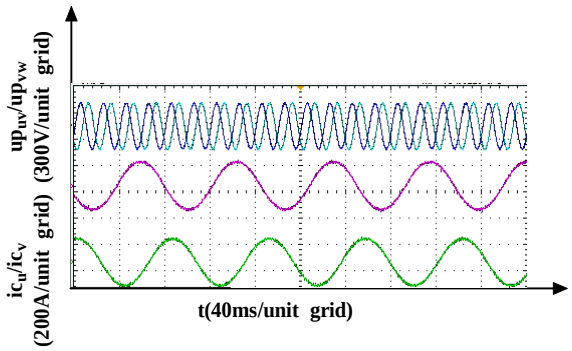

Fig. 7 (b). When rotor speed is 400 r/min, 30 kW resistance load steady-state output wave.

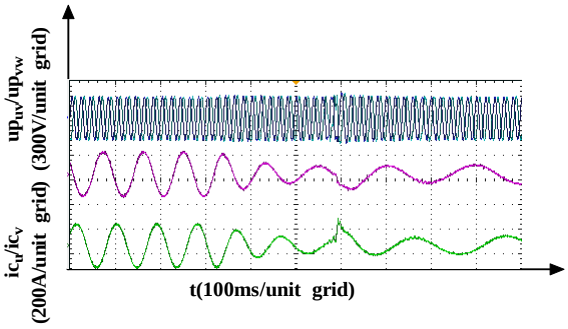

Fig. 7 (c). When rotor speed is 400 r/min, dynamic output wave when resistance load varying from 30 kW to 6 kW.

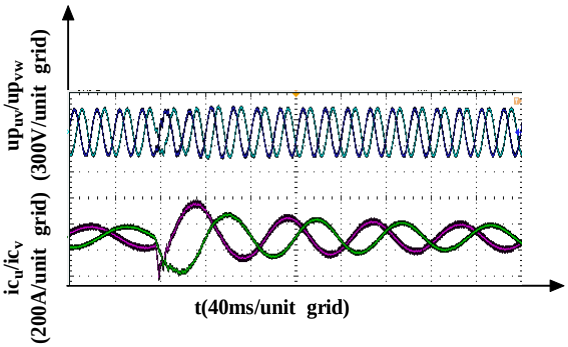

Fig. 7 (d). When rotor speed is 400 r/min, dynamic output wave when load varying from resistance load 6 kW to small motor load.

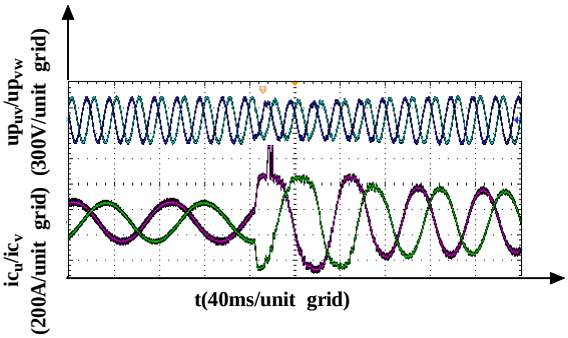

Fig. 7 (e). When rotor speed is 400 r/min, dynamic output wave when load varying from 24 kW resistance load to large motor load.

From Fig. 6, when rotor speed is 500 r/min (in synchronous state), power winding line voltage effective value still keeps constantly 400 V and frequency keeps 50 Hz whether there is load (Fig. 6 (b)) or not (Fig. 6(a)) if keeping the control current frequency equal to zero (giving control winding DC).

From Fig. 7, when rotor speed is 400 r/min (in sub-synchronous state), power winding line voltage effective value still keeps constantly 400 V and frequency keeps 50 Hz whether there is resistant load or motor load (in Fig. 7(b)-Fig. 7(d)) or not (in Fig. 7(a)) if adjusting the control current frequency in time to about 10 Hz by controlling the inverter (but

the phase sequence of the control winding is the same to that of the power winding).

According to Fig. 7(a), Fig. 7(b) and Fig. 7(c), when load increases (from no-load to 30 kW resistant load) or decreases (from 30 kW resistant load to 6 kW resistant load), control current increases or decreases correspondingly. whether small power motor load or large power motor load is connected with the BDFG (in Fig. 7(d)-Fig. 7(e)), there is a transient process, but power winding voltage amplitude and frequency is nearly invariable.

From Fig. 5-Fig. 7, when rotor speed is in sub-synchronous state, in synchronous state, or in super-synchronous state, power winding line voltage effective value still keeps constantly 400 V and frequency keeps 50 Hz (the same as the grid voltage amplitude and frequency) whether there is load or not if adjusting the control current frequency to proper value by controlling the inverter in time. According to Fig. 5-Fig. 7, when the experimental generator works at the three different modes, the output power winding voltage wave is nearly sinusoidal wave without harmonic content. When load increases or decreases, control current increases or decreases correspondingly. Whether small power motor load or large power motor load is connected with the BDFG, there is a transient process, but power winding line voltage amplitude and frequency is nearly invariable.

5. Conclusions

The Doubly-fed induction generator (DFIG) is widely applied in energy conversion systems such as wind turbines or pump-alike installations. However, the conventional DFIG requires brushes and copper slip-rings. A pole-changing wound rotor BDFM with an optimized rotor design is studied. It can be operated in sub-synchronous state and super-synchronous state if excited current is AC and also in synchronous state if excited current is DC through inverter absorbing grid energy or feeding back energy to grid whether in motor mode or in generator mode. The main advantages of this brushless and no-copper slip-rings machine is less maintenance, no noises and better stability. It has high utilization rate and lower harmonic content. In this paper, through modeling and simulation of BDFM, the simulation results show that BDFM can run in the three different speed mode whether as motor or as generator. When the rotor speed was varied from sub-synchronous speed to super-synchronous speed, its power winding output voltage wave is nearly sinusoidal wave without harmonic content and output voltage frequency and amplitude was nearly the same as that of the grid through controlling the control winding current (excited current) amplitude and frequency. Finally, experimental research was done based on 64 kW experimental BDFM prototype. Experimental research results verified the simulation conclusions.

Acknowledgements

This work has been funded by Hubei Provincial Natural Science Foundation of China (Grant No. 2013CFB023).

References

[1]. Roberto Cárdenas, Rubén Peña, Patrick Wheeler, Jon Clare, Andrés Muñoz, Alvaro Sureda, Control of a wind generation system based on a brushless doubly-fed induction generator fed by a matrix converter, *Electric Power Systems Research*, Vol. 103, 2013, pp. 49-60.

[2]. Huang Shou-Dao, Wang Yao-Nan, Wang Yi; Gao Jian, Study of active and reactive power control for brushless doubly-fed machine, *Zhongguo Dianji Gongcheng Xuebao/ Proceedings of the Chinese Society of Electrical Engineering*, Vol. 25, Issue 4, 2005, pp. 87-93.

[3]. Hamza Chaal, Milutin Jovanovic, Power control of brushless doubly-fed reluctance drive and generator systems, *Renewable Energy*, Vol. 37, Issue 1, 2012, pp. 419-425.

[4]. Bian Song-Jiang, He Yi-Kang, Pan Zai-Ping, Modeling and simulation of the cascade brushless doubly-fed machine, *Zhongguo Dianji Gongcheng Xuebao/Proceedings of the Chinese Society of Electrical Engineering*, Vol. 21, Issue 12, 2001, pp. 33-37.

[5]. S. Williamson, A. C. Ferreira, A. K. Wallace, Generalized theory of the brushless doubly-fed machine, Part 1: Analysis, *IEE Proceedings: Electric Power Applications*, Vol. 144, Issue 2, 1997, pp. 111-122.

[6]. Zhang Ai-Ling, Zhang Yang, Direct torque control for brushless doubly-fed machine based on torque predict control strategy, *Dianji Yu Kongzhi Xuebao/Electric Machines and Control*, Vol. 11, Issue 4, 2007, pp. 326-330.

[7]. Wang Leying, Xia, Chaoying, Filed oriented direct feedback control of cascaded brushless doubly-fed machine, *Zhongguo Dianji Gongcheng Xuebao/Proceedings of the Chinese Society of Electrical Engineering*, Vol. 31, Issue 30, 2011, pp. 132-139.

[8]. Wang Ai-Long, Xiong Guang-Yu, Computation of inductances of the brushless doubly-fed machine, *Zhongguo Dianji Gongcheng Xuebao/ Proceedings of the Chinese Society of Electrical Engineering*, Vol. 29, Issue 9, 2009, pp. 93-97.

[9]. Wang Ai-Long, Xiong Guang-Yu, Analysis of brushless doubly-fed machine by time stepping finite element method, *Zhongguo Dianji Gongcheng Xuebao/Proceedings of the Chinese Society of Electrical Engineering*, Vol. 28, Issue 21, 2008, pp. 123-127.

[10]. Richard McMahon, Peter Tavner, Ehsan Abdi, Paul Malliband, Darren Barker, Characterising brushless doubly fed machine rotors, *IET Electric Power Application*s, Vol. 7, Issue 7, 2013, pp. 535-543.

[11]. Xiong Fei, Wang Xuefan, Zhang Jingwei, Kan Chaohao, Chain equivalent circuit model of wound-rotor brushless doubly-fed machine, *Diangong Jishu Xuebao/Transactions of China Electrotechnical Society*, Vol. 25, Issue 2, 2010, pp. 15-21.

[12]. Kan Chaohao, Wang Xuefan, Xiong Fei, A brushless doubly-fed machine with star-circle rotor winding, *Zhongguo Dianji Gongcheng Xuebao/Proceedings of the Chinese Society of Electrical Engineering*, Vol. 31, Issue 3, 2011, pp. 111-117.

[13]. Kan Chaohao, Wang Xuefan, Operation range of brushless doubly-fed machine based on slot-harmonics, *Zhongguo Dianji Gongcheng Xuebao/ Proceedings of the Chinese Society of Electrical Engineering*, Vol. 31, Issue 24, 2011, pp. 124-130.

[14]. Kan Chaohao, Wang Xuefan, Design and testing of a 64 kW doubly-sine wound rotor brushless doubly-fed induction generator, *Zhongguo Dianji Gongcheng Xuebao/ Proceedings of the Chinese Society of Electrical Engineering*, Vol. 33, Issue 33, 2013, pp. 115-122.

[15]. Wang Xuefan, Wound-rotor brushless doubly-fed machine air-gap MMF wave, *Huazhong Keji Daxue Xuebao (Ziran Kexue Ban)/Journal of Huazhong University of Science and Technology (Natural Science Edition)*, Vol. 41, Issue 9, 2013, pp. 129-132.

[16]. Xiong Fei, Wang Xuefan, Cheng Yuan, Studies of brushless doubly-fed machines with an unequal-turn coil rotor structure, *Zhongguo Dianji Gongcheng Xuebao/Proceedings of the Chinese Society of Electrical Engineering*, Vol. 32, Issue 36, 2012, pp. 82-88.

[17]. Xiong Fei, Wang Xuefan, Design of a low-harmonic-content wound rotor for the brushless doubly fed generator, *IEEE Transactions on Energy Conversion*, Vol. 29, Issue 1, 2014, pp. 158-168.
